Parameterization of the LHCb magnetic field map

Adlène Hicheur, Géraldine Conti

Ecole Polytechnique Fédérale de Lausanne, Lausanne, Switzerland

E-mail: Adlene.Hicheur@cern.ch,geraldine.conti@epfl.ch

Abstract. The LHCb warm magnet[1] has been designed to provide an integrated field of 4 Tm for tracks coming from the primary vertex. To insure good momentum resolution of a few per mil, an accurate description of the magnetic field map is needed. This is achieved by combining the information from a TOSCA-based simulation and data from measurements. The paper presents the fit method applied to both the simulation and data to achieve the requirements. It also explains how the corresponding software tool is integrated in the LHCb Gaudi software and shows the relation with the environment in which it is used.

1. Introduction

Initial studies of the field map were done using a grid of values generated by a TOSCA simulation and measurements performed with Hall probes[2]. Comparisons have shown that, although the simulation accounts correctly for the measurements, some mismatch between simulated field and data can be observed in several regions and in particular, near the first Cherenkov light detector (RICH1) and in the magnet region. On the other hand, technical limitations related to the probes positioning did not allow obtaining measurements in the full acceptance.
To derive a realistic field map covering all the regions, we implemented a three dimensional fit to the TOSCA field values, using a development in series of basis functions. The set of basis functions is optimized by the mean of a Gram-Schmidt orthogonalization procedure which keeps only the terms that significantly reduce the least square[3].We then compare the parameterization and the measurements and fit correction terms. Regions where no data is available are described by extrapolating the corrective functions.

2. Available input for the map determination

The information we use to determine the field map comes from two sources:

- A TOSCA simulation relying on finite element calculations (figure 1) providing field values positioned on 10 cm cubic cells, resulting in about 180000 numbers for each field component.
- Measurements performed in late 2005 [2]. These measurements were taken by sixty Hall probes disposed into a two planes grid-configuration (figure 2) moving on a rail along the beam (z) axis. The grid could be moved in several positions in the transverse (xy) plane as well (figure 3).

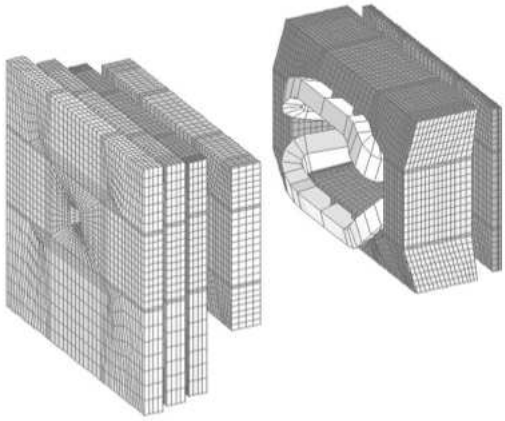

Figure 1. TOSCA representation of the magnet, hadron calorimeter and muon shields, based on Finite Elements calculation method.

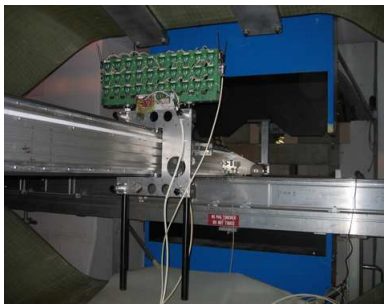

Figure 2. Planes supporting the Hall probes used for the magnetic field measurement.

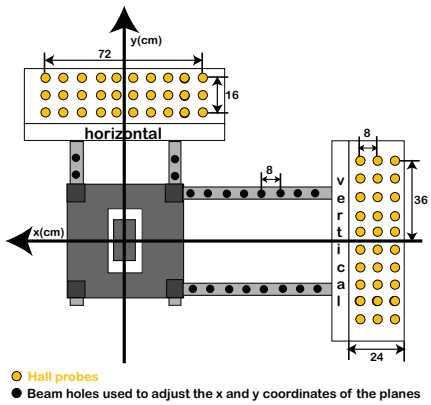

Figure 3. Drawing showing the Hall probes positions in the measurements planes and the rails system used for the transverse scan.

3. The fitting techniques

To determine the field map, we have envisaged several approaches that are technically different in their implementation but are fundamentally correlated in their philosophy.

3.1. Three dimensional interpolation

Given the set $\mathbf{\Omega}_{sim}$ of field values $\mathbf{B}_{sim}$ provided by the simulation and the set $\mathbf{\Omega}_{meas}$ of measurements $\mathbf{B}_{meas}$, we first set up a global interpolation strategy in which we minimize the estimator:

$$\Im = \lambda_1 \sum_{i,\mathbf{\Omega}_{sim}} (\mathbf{B}_{sim}(\vec{x}_i) - \mathbf{f}(\vec{x}_i))^2 + \lambda_2 \sum_{j,\mathbf{\Omega}_{meas}} (\mathbf{B}_{meas}(\vec{y}_j) - \mathbf{f}(\vec{y}_j))^2 \qquad (1)$$

λ_1 and λ_2 are weights (in the general case, they can be set to be position-dependent). $\mathbf{f}$ is a function build as follows:

$$\mathbf{f}(\vec{z}) = \sum_{\vec{k}\in\mathbb{Z}^3} c(\vec{k})\phi(\frac{\vec{z}}{L} - \vec{k}) \tag{2}$$

$c(\vec{k})$ are coefficients to be determined and $\phi(\vec{u})$ are Kernel functions used for the interpolation (typically three dimensional cubic splines). L is the typical cell size for which the interpolation is computed.
To regularize the interpolation, a smoothing term is added to the criterion 1 to prevent local oscillation effects.
Although the method is generic, it requires the simultaneous fit of a large number of $c(\vec{k})$ coefficients ($O(10^6)$). We thus decided to adopt a simplified strategy in which we proceed to a three dimensional polynomial fit.

3.2. Three dimensional fit
In this method, we consider the following development:

$$f(\vec{x}_i) = \sum_l c_l m_l(\vec{x}_i) \tag{3}$$

c_l are coefficients to be determined in the fit and m_l are functions forming the fitting basis. For a simple polynomial basis, $m_l(x_i, y_i, z_i)$ is of the form $x_i^a y_i^b z_i^c$.
In our case, we chose Chebychev monomials[1], the $m_l(x, y, z)$ functions being of the form $T_m(x)T_n(y)T_p(z)$, where $T_k(u)$ is the k^{th} order Chebychev polynomial for the variable u. We recall the recurrence relation linking subsequent orders:

$$\begin{aligned} T_{k+1}(u) &= 2uT_k(u) - T_{k-1}(u) \\ T_0(u) &= 1 \\ T_1(u) &= u \end{aligned} \tag{4}$$

The goal is then to determine the optimized number of terms and c_l coefficients in equation 3 such that following sum of squared residuals is minimized:

$$S = \sum_i (f(\vec{x}_i) - B_i)^2 \tag{5}$$

After setting the maximum number of terms for each dimension, the procedure (see [3, 5] for the details) consists in two steps:

- Choice of the optimal combination of terms through a Graam-Schmidt orthogonalization procedure in which the functions are selected according to their minimization power in equation 5.
- Determination of the c_l coefficients through a standard least square fit.

To achieve the target precision, we were forced to divide the fitting volume into sub-regions. This can be seen as a compromise with respect to the full interpolation procedure (previous paragraph) for which each cell is a sub-region. With this, we reduce the number of coefficients by three orders of magnitude.

[1] The Chebychev polynomials are known to be the best approximation polynomials for continuous functions. In particular, they minimize the nasty oscillation effects (called Runge's phenomenon) observed for high-order polynomial fit/interpolation [4].

4. Fit regions

Due to the complexity of the B field behaviour, several regions of parameterization have been defined. The boundary choice results from a compromise between three requirements : achieving the target precision, minimizing the number of regions and the number of terms in the paramtererizations of each region.

The choice of the cuts is driven by the field variations. Regions where the field gradients are big will be smaller and will require more terms in the parameterizations than the ones where the field variations are smoother. We have simplified the regions definitions by relying on the z coordinate only for the three B field components. We obtained fifteen regions (figure 4), with boundaries at z = 100, 150, 200, 240, 300, 410, 470, 510, 610, 670, 730, 800, 850 and 900 cm. The locations of these cuts do not systematically correspond to physical positions of subdetectors.

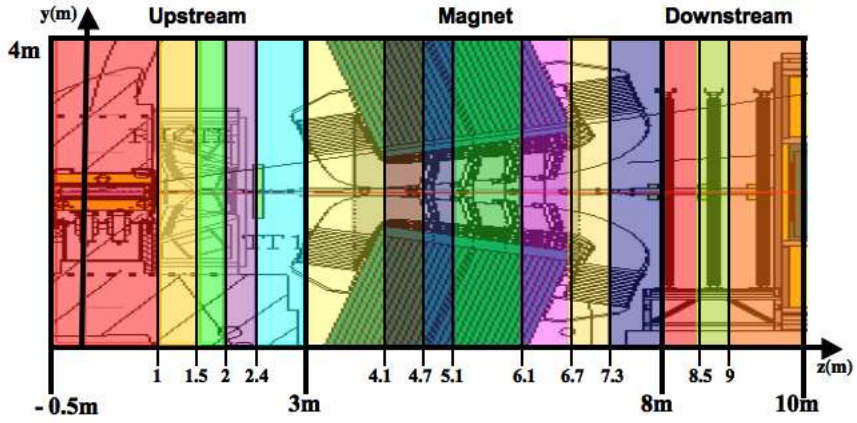

Figure 4. Positions of the z cuts separating the fit regions (black lines) along with the delimitations of the upstream, magnet and downstream sectors (thick black lines).

Inside the magnet, quick variations of the field are observed close to the magnet coils. In order to obtain parameterizations with a reasonable number of terms (up to O(150)), the region [y_{edge}-30cm,y_{edge}] has been fitted separately.

5. Fit results

The fit has been performed using the ROOT software [6]. The analytic caculations for the B_x, B_y and B_z components show a very good matching with the TOSCA simulated values for all the sectors. The reached precision is O(10^{-3}). Figure 5 shows examples of comparisons between TOSCA-based numbers and analytic values.

The relative discrepancy between the parameterizations of the adjacent regions has been studied and found to be of the same order of the fit precision for each magnetic component.
Matching with data is then performed by parameterizing (using the same basis of functions) the residuals between the analytic field determination and the measurements. Figure 6 shows examples of such residuals distributions.

The final parameterization is derived by combining the initial one and the residual parameterization. Figure 7 shows the effect of correcting the parameterized simulation with the residuals.

In the regions where no measurement is available, the idea is to extrapolate residual parameterizations, taking into account boundary conditions as well as constraints from Maxwell equations.

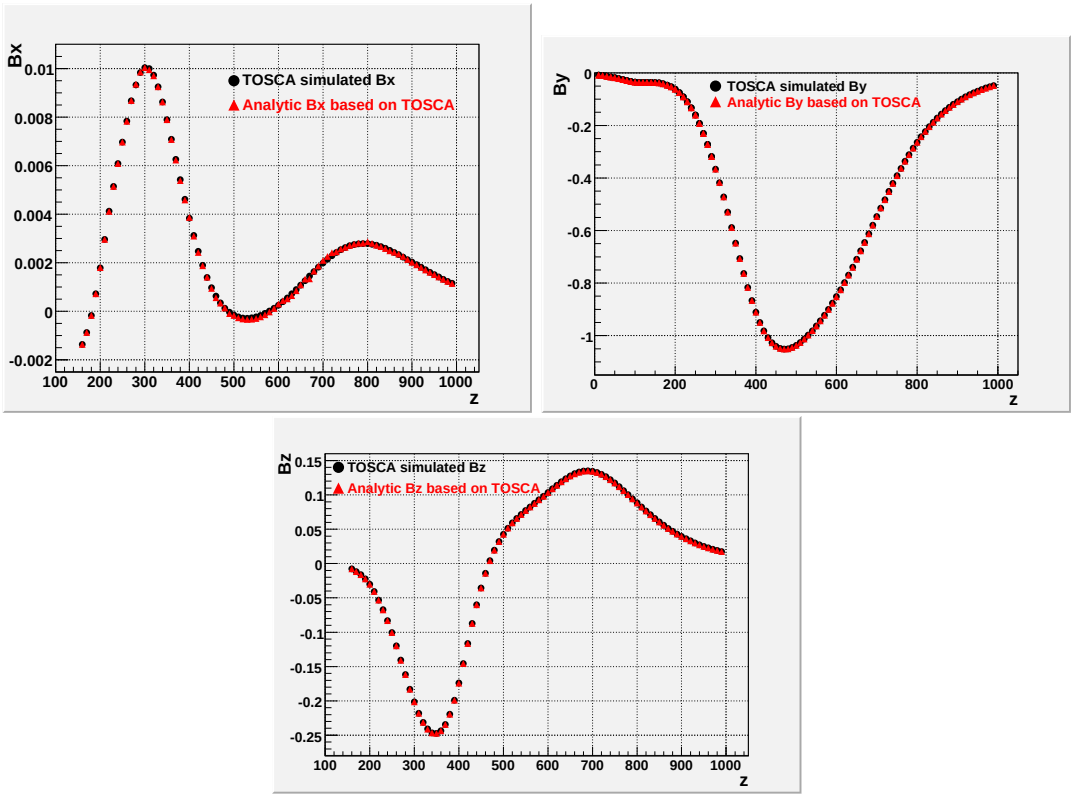

Figure 5. Plots of the variations as a function of z of the magnetic field components B_x (for $x = 40$ cm, $y = 40$ cm), B_y (for $x = 0$ cm, $y = 0$ cm) and B_z (for $x = 40$ cm, $y = 40$ cm).

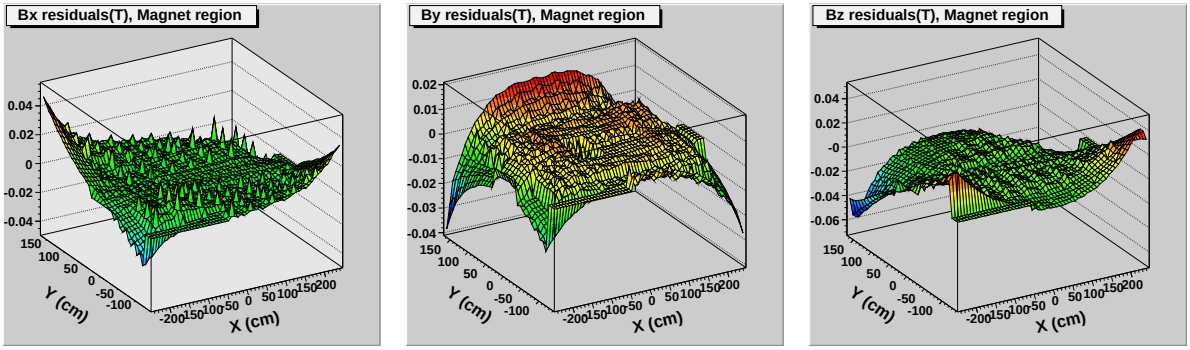

Figure 6. Data-(Parameterized simulation) residuals for the three field components in the magnet region.

This scheme is still under study.

6. Embedding in LHCb software

The parameterized determination of the field vector for a given position has required the implementation of a service in the Gaudi framework [7]. This service must be initialized by configuration scripts, if any of the user algorithms requires the field. For a given position, the magnetic field components are obtained through the call to a generic method, fieldVector, which

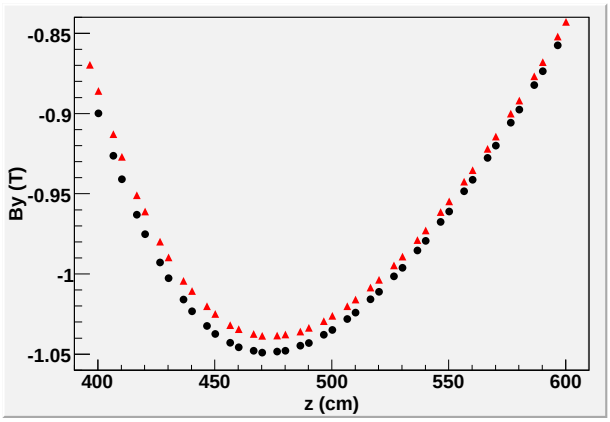

Figure 7. Plot of the B_y component as a function of z (for $x = 100$ cm, $y = 4$ cm). The filled circles represent the simulation while the triangles represent the final parameterization including the matching with data. The z slice $400 - 600$ cm has been chosen to illustrate a region where the difference is easily visible.

in turn calls the region determination method and finally the analytic calculation is performed. Figure 8 depicts the working principle of how the service is called by a generic Gaudi algorithm.

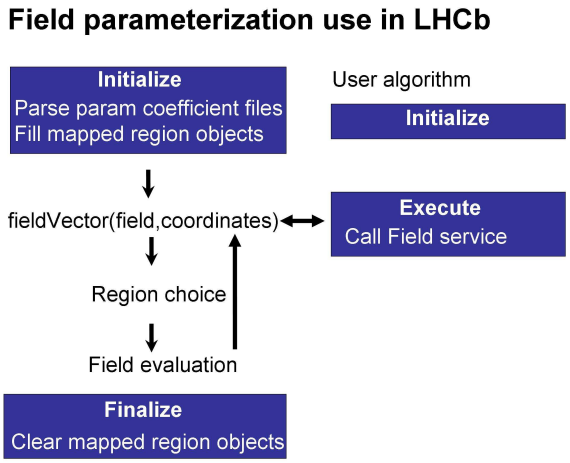

Figure 8. Typical example of use of the parameterized field service by a user algorithm. The diagram shows the service methods flow when a call is done.

7. Validation tests

To validate the parameterization of the field map, we implemented several tests in increasing order of complexity. We first compared the results for the field components between the parameterized determination and the one performed by a linear interpolation of the TOSCA grid values, as shown in figure 5. In a second step, we made the same comparison for the bending vector:

$$\int \vec{B} \times d\vec{l} \tag{6}$$

In this exercise, we generated a set of segments originating from the origin $(0, 0, 0)$ (theoretical "primary vertex") with a random distribution of x (dx/dz) and y (dy/dz) slopes, within the LHCb acceptance, ± 300 mrad and ± 250 mrad, respectively. We then compute the component of the bending vector, for each segment, between the origin point and the coordinate (0,0,900) cm, i.e, after the magnet. Figure 9 shows the three components of the bending vector for the linear interpolation method and the parameterization.

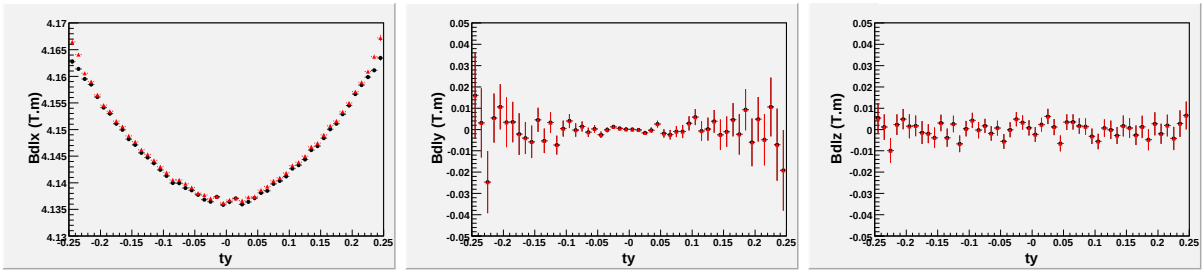

Figure 9. Profile plots of the three bending vector components, as a function of the y slope of the generated segments. Dots and triangles represent the linear interpolation and parameterized representation, respectively.

One can see that the two representations match in most cases except for the x component of the bending vector where a small discrepancy is observed for high values of the y slope: this corresponds to the high $|y|$ region, mentioned in paragraph 4, where the field gradient is more important. After investigating, we were able to figure out that due to the smaller number of points used for the parameterization of this region, the resulting fit is less accurate. To solve that, we changed the y edge region definition such that it overlaps with the central region.
Finally, we tested the analytic field description by using it in the track reconstruction and comparing it to the TOSCA linear interpolation. We ran on few $B_d \to J/\psi K_S$ events: figure 10 shows the results for the resolutions of track parameters. We can observe that the two field descriptions give similar results.

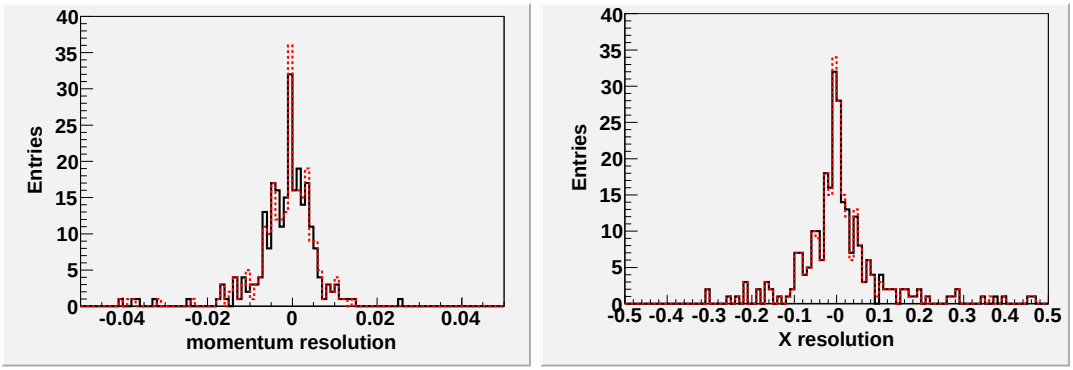

Figure 10. Plots of the momentum and X track parameter resolutions at the vertex. The solid and dashed lines represent the histograms for the linear interpolation and parameterized representation, respectively.

8. Conclusion

An analytic representation of the LHCb magnetic field map has been implemented. The optimized multidimensional fit applied to derive the parameterization allowed us to achieve the target precision. For the purpose of testing, this functional mapping has been ported to the framework of the LHCb software. With the validation tests, we were able to both tune the parameterization and check the quality of the tracking performance. The inclusion of corrections from real measurements has been successfully achieved in areas where the parameterized simulation and measurements overlap. Where no measurement is available, a correction scheme including constraints from Maxwell equations has been considered and is still being studied.

References

[1] *LHCb Magnet*, Technical Design Report, CERN/LHCC/2000-007, December 1999.

[2] *Tests and Field Map of LHCb Dipole Magnet*, M.Losasso et al., IEEE Transactions on Applied Superconductivity, Volume 16, Issue 2, pages 1700-1703, June 2006.

[3] H.Wind, Yellow Report 72-21, CERN, 1972. H.Wind, Yellow Report, EP/81-12, CERN, 1981.

[4] C.Lanczos, *Applied Analysis*, Prentice-Hall, Inc., Engelwood Cliffs, NJ, 1956.

[5] LHCb note 2007-093, A.Hicheur, G.Conti (2007).

[6] R.Brun, F.Rademakers, *ROOT - An Object Oriented Data Analysis Framework*, Proceedings AIHENP'96 Workshop, Lausanne, Sep. 1996, Nucl. Inst. & Meth. in Phys. Res. A 389 (1997) 81-86. See also http://root.cern.ch/.

[7] Barrand G. et al., *GAUDI - A software architecture and framework for building LHCb data processing applications*, Proceedings of CHEP 2000.